Nonequilibrium Molecular Dynamics Simulation Study on the Shear-Induced Orientational Change of Rodlike Molecules

Changjun Lee, Hoon-goo Sim, Woonchun Kim, Song Hi Lee,† and Hyungsuk Pak*

Department of Chemistry, Seoul National University, Seoul 151-742, Korea
†Department of Chemistry, Kyungsung University, Pusan 608-736, Korea
Received January 11, 2000

We present the results of computer simulation for the steady shear flows of rodlike molecules using nonequilibrium molecular dynamics simulation (NEMD) method. The model particle is a rigid rod composed of linearly connected 6-sites and the Lennard-Jones 12-6 potential governs interactions between sites in different molecules. The system of rodlike molecules exhibits the change of orientational structure, that is, isotropic-nematic transition at high shear rates. We elucidate the nature of the ordered system developed from an isotropic phase by steady shear through an analysis of various quantities: orientational order parameters, orientational pair correlation functions, orientational distribution function, and snapshots of configurations. The effects of temperature and density on the shear rate dependence of orientational structure are described.

Introduction

Liquid crystalline materials typically involve organic compounds and show a state of order intermediate between the familiar crystal and isotropic liquid. Liquid crystals (LCs) may be divided into two main categories, that is, thermotropic and lyotropic LC: thermotropic LC has temperature-dependent phase behavior, while lyotropic LC exhibits concentration-dependent phase behavior. This mesomorphic state is distinguished from other condensed phases by the existence of orientational order among their constituent molecules. In reality, without an external constraint the mesomorphic phase has no macroscopic long-range order because the director varies continuously throughout a liquid crystal sample. However, the application of an external field, such as a magnetic field, produces macroscopic alignment of the director.[1] It implies that significant structural change can occur in liquid crystals due to applied fields: an electric field, a magnetic field, a mechanical force, or a surface effect at the boundary.[2-4]

There have been many investigations of the alignment of nematic liquid crystalline materials by either a magnetic field or an electric field.[5] There have also been several studies of the effect of applying two constraints to a nematic sample, such as an electric field and a surface constraint. As a result, the basic features of these hydrodynamic processes have been characterized, and successful theoretical models based on continuum theory have been developed to describe the phenomena.[2,3]

NEMD simulation[6(a)-(c)] has played a key role in our understanding the rheological behaviors of complex fluids, such as liquid crystals[6(c)] and polymers.[6(d)] Recently, Bennett *et al.*[7] have studied the anisotropy of the viscosity and shear-induced structural changes in perfectly oriented liquid crystals *via* NEMD simulation. They used two models for the shear-induced transition from smectic to nematic phase: perfectly oriented Gay-Berne particles and anisotropic soft spheres.

The main purpose of this work is to study the basic features of the field-induced alignment process for anisotropic molecules which can form liquid crystalline phase. In the present work, we focus on the shear-induced isotropic-nematic transition, and the effects of density and temperature on the shear rate dependence of orientational structure. We have performed computer simulation for the steady-shear flows of rodlike molecules using NEMD method. We present our extensive simulation results of the shear-induced structural changes from an isotropic fluid to nematic phase.

The organization of this paper is as follows: Section II contains a description of our model and simulation method. We present the results of our simulation and discussion in section III and concluding remarks are given in section IV.

Model and Simulation Method

The molecular system studied here consists of rigid rod molecules. The model particle is a rigid rod composed of linearly connected 6-sites and the Lennard-Jones 12-6 potential (that is, $u^{LJ}(r_{ij}) = 4\varepsilon((\sigma/r_{ij})^{12}-(\sigma/r_{ij})^{6})$) governs interactions between sites in different molecules. The potential and molecular parameters used in this study are as follows: $\sigma = 0.2615$ nm, $\varepsilon = 0.5986$ kJ/mol, the distance between the first and last site of a molecule $l = 0.702$ nm, and the mass of a molecule $m = 78.12$ g/mol.

In this study, we use a canonical ensemble with fixed *N*(number of molecules), V(volume of system), and T(temperature). Gauss's principle of least constraint is used to maintain the system at a constant temperature. For the study of planar Couette flow, in which fluids are subjected to homogeneous shear between two parallel plates, it is convenient to apply the SLLOD equations of motion.[6(a)] They are an exact description of steady planar Couette flow arbitrarily far from equilibrium. For uniaxial rigid molecules, the SLLOD equations of motion are given by

$$\frac{d\mathbf{r}_i}{dt} = \frac{\mathbf{p}_i}{m} + \mathbf{e}_x \gamma y_i, \tag{1}$$

$$\frac{d\mathbf{p}_i}{dt} = \mathbf{F}_i - \mathbf{e}_x \gamma p_{yi} - \alpha \mathbf{p}_i \tag{2}$$

$$\mathbf{I}_{pi} \cdot \frac{d\boldsymbol{\omega}_{pi}}{dt} + \boldsymbol{\omega}_{pi} \times (\mathbf{I}_{pi} \cdot \boldsymbol{\omega}_{pi}) = \boldsymbol{\Gamma}_{pi}. \tag{3}$$

Here, $\mathbf{r}_i$ and $\mathbf{p}_i$ are the position and momentum of center of mass of molecule i, respectively. $\mathbf{e}_x$ is a unit vector in the x-direction, and $\mathbf{F}_i$ is the force exerted on molecule i due to interaction with other molecules through the pairwise site-site interactions. $\gamma(=\partial u_x/\partial y)$ is a shear rate, that is, the xy-plane is defined as the shear plane in this study. $\mathbf{I}_{pi}$ and $\boldsymbol{\omega}_{pi}$ denote the moment of inertia tensor and the angular velocity in the principal axis frame of molecule i, respectively. In this study, we regard the component of principal moments of inertia around the symmetry axis of a molecule, I_{zz}, as zero. The principal torque exerted on molecule i due to interaction with other molecules is denoted as $\boldsymbol{\Gamma}_{pi}$.

The omitted relation between $\boldsymbol{\omega}_{pi}$ and the rate of change of a molecular symmetry axis $d\hat{\mathbf{u}}_i/dt$, is implemented in terms of the quarternions.[8] For a detailed description of the rotational equations of motion, we refer to the classic textbook.[9]

The Gaussian thermostat multiplier α, which makes the peculiar translational kinetic energy a constant of motion, is determined by

$$\alpha = \frac{\sum_{i=1}^{N} (\mathbf{F}_i \cdot \mathbf{p}_i - \gamma p_{xi} p_{yi})}{\sum_{i=1}^{N} \mathbf{p}_i \cdot \mathbf{p}_i}. \tag{4}$$

This thermostat does not exert any torque on the molecules or the director and consequently it does not affect the shear-induced alignment or rotation. The isokinetic equilibrium equations of motion are recovered by setting $\gamma = 0$ in Eqs. (1) and (2).

A cubic simulation box with Lees-Edwards homogeneous shear boundary condition,[10] well known as a sliding brick boundary condition, was used in all the calculations. Simulations were carried out over a wide range of shear rate: 10^{-3} $ps^{-1} < \gamma < 8$ ps^{-1}. A spherical cut-off radius r_c was set at 0.5 L (L is the length of cubic box) for all pairwise interactions. We adopted the Gear's fifth-order predictor-corrector algorithm[11] for the integration of equations of motion. The time step Δt was used from 1 fs to 0.125 fs depending on the shear rate for a transient period.

The orientational distribution of system can be fully described by orientational distribution function (ODF).[12] At least in principle, scattering methods give information on the full ODF, but experimentally it is very difficult to determine the full ODF. So one often resorts to an expansion of this function. The ODF can formally be expanded in terms of a complete basis set. For system composed of molecule with cylindrical symmetry and having a uniaxial phase symmetry, the ODF is expressed as

$$f(\theta) = \sum_{n=0}^{\infty} \frac{4n+1}{2} \langle P_{2n}(\cos\theta) \rangle P_{2n}(\cos\theta). \tag{5}$$

Here θ is the angle between symmetry axis of molecule and the director $\mathbf{n}$ describing the average direction of alignment for molecules, and P_L denotes a Legendre polynomial with rank L.

During the simulation, the orientational order was monitored through the order parameters S_{2n} ($= \langle P_{2n}(\cos\theta) \rangle$, n = 1, 2, 3). Since the direction of $\mathbf{n}$ is not known *a priori*, the order parameter S_2 has to be determined using another approach.[12] In the present work, S_2 is associated with the largest eigenvalue obtained through the diagonalization of the ordering tensor

$$Q_{\alpha\beta} = \frac{1}{N} \sum_{i=1}^{N} \left(\frac{3}{2} u_{1\alpha} u_{1\beta} - \frac{1}{2} \delta_{\alpha\beta} \right) \quad (\alpha, \beta = x, y, z). \tag{6}$$

Here, $u_{i\alpha}$ is α-component of the orientational unit vector of a molecule i, and $\delta_{a\beta}$ is the Kronecker δ-symbol. The eigenvector associated with the largest eigenvalue provides the director $\mathbf{n}$. By definition, the value of S_2 in the isotropic phase is 0, whereas it will tend to be 1 in a highly ordered phase. But the value of S_2 obtained by simulation remains to be small finite value in isotopic phase due to finite system size. Other order parameters with higher order can be calculated straightforwardly after the determination of director vector.

Another useful quantity for elucidating the nature of orientationally ordered systems is orientational pair correlation functions (OPCFs).[12] The OPCFs are defined by

$$g_L(r_{ij}) = \langle P_L(\cos\theta_{ij}(r_{ij})) \rangle \qquad (L = 2, 4, 6), \tag{7}$$

where $\theta_{ij}(r_{ij})$ is the angle between molecular axes $\mathbf{u}_i$ and $\mathbf{u}_j$ of molecules i and j with *inter*-particle distance r_{ij}.

Results and Discussion

Throughout the simulation, the order parameter S_2 was monitored from onset of steady shear on an isotropic system to obtain meaningful samples for the steady state. The time step used to integrate the equations of motion was in most cases set at 1 fs; as for high shear rates ($\gamma \geq 4.0$ ps^{-1}), we set time step at 0.025 fs or 0.0125 fs during a transient period. Figure 1(a) shows the characteristic response of rigid molecules to the applied steady shear. For the sake of clarity, we represent the evolution of S_2 from onset of steady shear for 100 ps at 300 K and 1.386 g/cm^3 at the following shear rates: $\gamma = 2.0$, 0.2, 0.001 ps^{-1}. Figure 1(b) reveals the evolution of S_2 over 100 ps for two states started from different initial orientational states under shear rate $\gamma = 2.0$ ps^{-1} at 300 K and 0.994 g/cm^3. Comparison was made between the results for the two states to investigate the possible effect of initial state on the steady states at Table 1. Configurations of every 10 fs interval for the last 50 ps periods were taken. The simulation results of Lennard-Jones energy per particle (E^{LJ}/N), shear viscosity ($\eta = -(P_{xy} + P_{yx})/2\gamma$, P_{xy} is the xy-component of a pressure tensor), and orientational order parameters show good

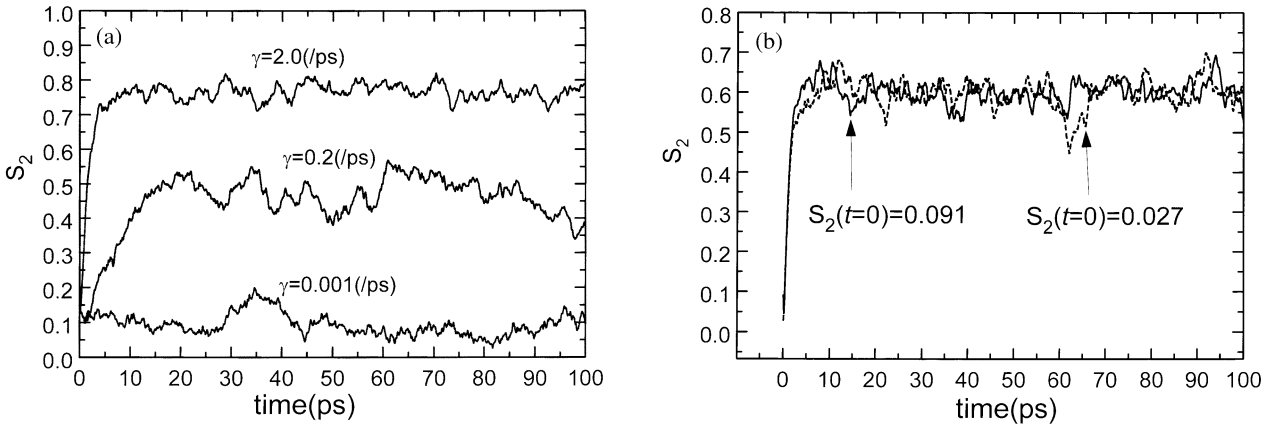

Figure 1. (a) The evolution of order parameter S_2 over 100 ps^{-1} from onset of steady shear at 300 K and 1.386 g/cm^3 for γ= 2.0, 0.2, 0.001 ps^{-1}. (b) The evolution of order parameter S_2 for two states started from different initial orientational order at 300 K, 0.994 g/cm^3, and shear rate γ= 2.0 ps^{-1}.

Table 1. The simulation results for two states started from different initial order parameters at 300 K, 0.994 g/cm^3, and $\boldsymbol{\gamma}$= 2.0 ps^{-1}. E^{LJ} is the Lennard-Jones energy, η denotes a shear viscosity, and <⋯> means an ensemble average. The Figures in parentheses are estimated (one standard deviation) errors in the quoted digits

S_2 (t=0)	$\langle \mathbf{E}^{LJ}/N \rangle$ (kJ/mol)	$\langle \eta \rangle$ (atm ps)	$\langle S_2 \rangle$	$\langle S_4 \rangle$	$\langle S_6 \rangle$
0.027	–16.582(0.291)	57.020(13.254)	0.608(0.038)	0.303(0.036)	0.131(0.030)
0.091	–16.597(0.348)	57.918(13.325)	0.604(0.025)	0.300(0.035)	0.129(0.032)

Table 2. The shear rates dependence of LJ-energy and order parameters for two states with different densities at 300 K. The number of molecules is 256. The Figures in parentheses are estimated (one standard deviation) errors in the quoted digits

ρ (g/cm^3)	γ (ps^{-1})	$\langle \mathbf{E}^{LJ}/N \rangle$ (kJ/mol)	$\langle S_2 \rangle$	$\langle S_4 \rangle$	$\langle S_6 \rangle$
1.386	0.000	-22.559(0.199)	0.088(0.027)		
	0.001	-22.538(0.216)	0.082(0.029)		
	0.010	-22.529(0.195)	0.127(0.046)		
	0.020	-22.558(0.189)	0.143(0.036)		
	0.040	-22.687(0.190)	0.255(0.025)		
	0.060	-22.709(0.159)	0.326(0.043)		
	0.070	-22.773(0.238)	0.301(0.061)		
	0.080	-22.645(0.200)	0.267(0.048)		
	0.100	-22.729(0.185)	0.350(0.029)	0.083(0.035)	0.018(0.027)
	0.200	-22.867(0.227)	0.443(0.062)	0.172(0.033)	0.061(0.026)
	0.400	-22.953(0.240)	0.542(0.044)	0.220(0.047)	0.071(0.032)
	0.600	-22.952(0.236)	0.609(0.037)	0.306(0.043)	0.136(0.035)
	0.800	-22.883(0.184)	0.632(0.038)	0.322(0.047)	0.142(0.042)
	1.000	-22.903(0.250)	0.669(0.032)	0.369(0.042)	0.179(0.042)
	2.000	-22.317(0.306)	0.754(0.025)	0.467(0.035)	0.248(0.037)
	4.000	-20.602(0.519)	0.836(0.013)	0.595(0.025)	0.374(0.031)
	8.000	-15.764(1.591)	0.891(0.011)	0.703(0.020)	0.503(0.028)
0.994	0.000	-17.233(0.234)	0.066(0.018)		
	0.001	-16.933(0.398)	0.069(0.018)		
	0.010	-17.000(0.330)	0.070(0.022)		
	0.100	-16.737(0.249)	0.106(0.031)		
	0.200	-17.080(0.408)	0.178(0.041)		
	0.400	-17.346(0.427)	0.303(0.032)		
	0.600	-17.033(0.281)	0.356(0.059)	0.107(0.049)	0.027(0.031)
	0.800	-17.173(0.346)	0.441(0.041)	0.154(0.033)	0.048(0.026)
	1.000	-16.993(0.308)	0.456(0.028)	0.165(0.030)	0.048(0.030)
	2.000	-16.621(0.313)	0.611(0.040)	0.311(0.042)	0.136(0.036)
	4.000	-16.041(0.308)	0.748(0.022)	0.481(0.026)	0.278(0.028)
	8.000	-15.111(0.569)	0.856(0.015)	0.655(0.025)	0.461(0.031)

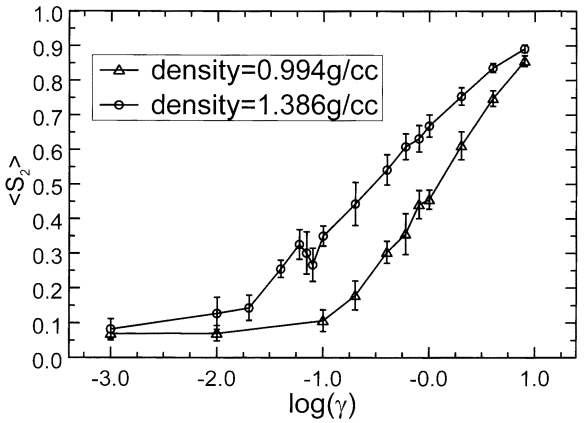

Figure 2. The variations of order parameter S_2 versus shear rate for two states having the densities of 0.994 and 1.386 g/cm^3, respectively. Temperature is 300 K and the number of particles is 256. The error bar denotes an estimated error (one standard deviation) for the mean value of data.

agreements between the two states.

The results for two state points having different densities under various shear rates at 300 K are contained in Table 2. We discarded the preliminary data ranged from the 100 ps^{-1} for shear rates ($\gamma \leq 2.0$ ps^{-1}) to 20 ps^{-1} for high shear rates ($\gamma \geq 4.0$ ps^{-1}). Time step used was in general set at 1 fs, for which consistent results could be obtained. Configurations of every 10 fs interval for 50 ps were taken to compare the stability of the system at various shear rates. More extensive calculation was carried out for the dense state.

Figure 2 shows the order parameter of the two states as a function of shear rate. The line in this figure was drawn for the guideline of eye. We can see the growth of orientational order with an increase of shear rate from Figure 2. The results for the dense system at moderate shear rates ($0.06 \leq \gamma \leq 0.08$ ps^{-1}) reveal slight deviations from this general trend, and exbihit large fluctuations. It may be associated with the pre-nematic behavior. In general, liquid crystalline systems response to temperature or concentration of solution in an abrupt manner, that is, the change of orientational or positional order is abrupt at a certain transition point. Unlike this feature, we observe the gradual growth of orientational order with an increase of shear rate in Figure 2.

For clarity, we depict the behaviors of OPCFs for representative three states in Figure 3: the isotropic phase ($\gamma = 0$), $\gamma = 0.1$, and 2.0 ps^{-1} at 300 K and 1.386 g/cm^3. As we can see Figure 3(a), the orientational order of the isotropic phase is clearly disappeared within short range. For $\gamma = 0.1$ ps^{-1} as shown in Figure 3(b), the remaining value of $g_2(r)$ implies that orientational order persists within the simulation length scale. Figure 3(c) clearly shows that a long-range orientational order is developed for shear rate $\gamma = 2.0$ ps^{-1}. Figure 3(d) depicts the $g_2(r)$ as a function of shear rate. (Note the graphs correspond to the following shear rates from top to bottom: $\gamma = 0.6$, 0.4, 0.2, 0.1, 0.06, 0.07, 0.08, 0.01, 0.001 ps^{-1}).

The behaviors of ODFs for $\gamma = 0.01$, 0.2, 1.0, and 4.0 ps^{-1}

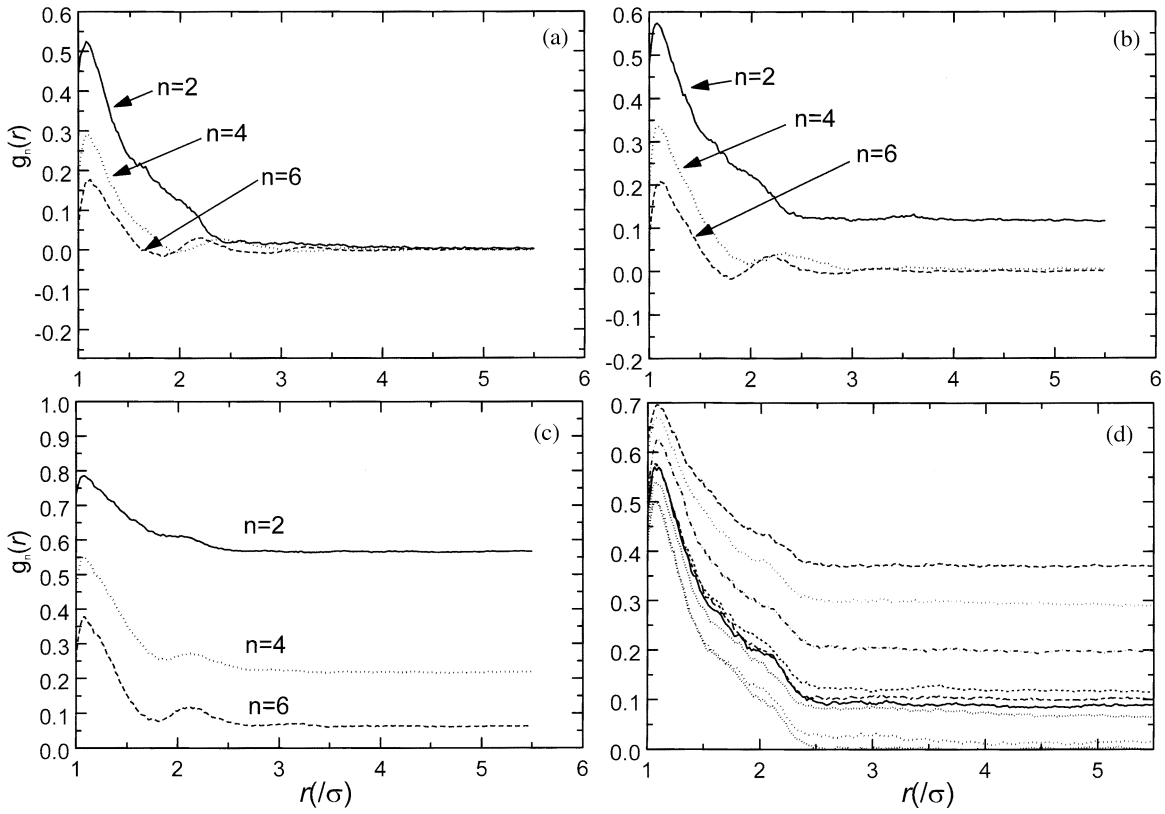

Figure 3. The variations of OPCFs at 300 K and 1.386 g/cm^3 for shear rate (a) $\gamma = 0$ ps^{-1} (an isotropic fluid), (b) $\gamma = 0.1$ ps^{-1}, (c) $\gamma = 2.0$ ps^{-1}. (d) $g_2(r)$ as a function of shear rate. From top to bottom, the shear rates are $\gamma = 0.6$, 0.4, 0.2, 0.1, 0.06, 0.07, 0.08, 0.01, and 0.001 ps^{-1}.

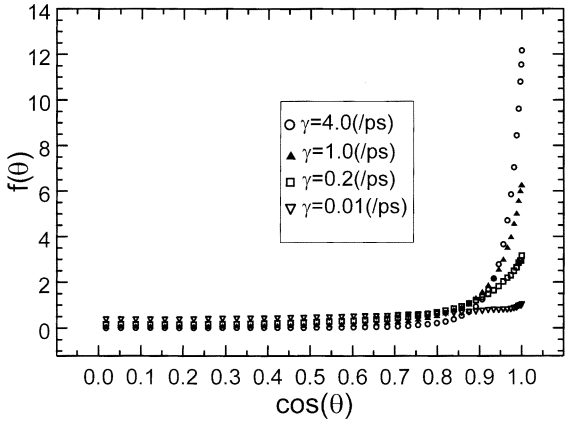

Figure 4. The ODF as a function of shear rate. For clarity, the ODFs are depicted for the following shea rates: γ= 4.0, 1.0, 0.2, and 0.01 ps^{-1}.

as shown in Figure 4, reveal the change of orientational distribution as a function of shear rate. It proves that nematic order is developing as shear rate rises. Figure 5 depicts the snapshots projected to each plane for γ= 8.0 ps^{-1} at 300 K and 1.386 g/cm^3. The projections to *xy*- and *xz*-plane indicate the nematic order along *x*-axis (the direction of director and shear flow). The *yz*-projection shows no clear positional or orientational order along the director, such as, hexagonal packing. From the similar analysis for the configurations of each shear rate, we finally concluded that no additional change of structure is found.

As shown in Figure 2, density affects the shear rate depen-

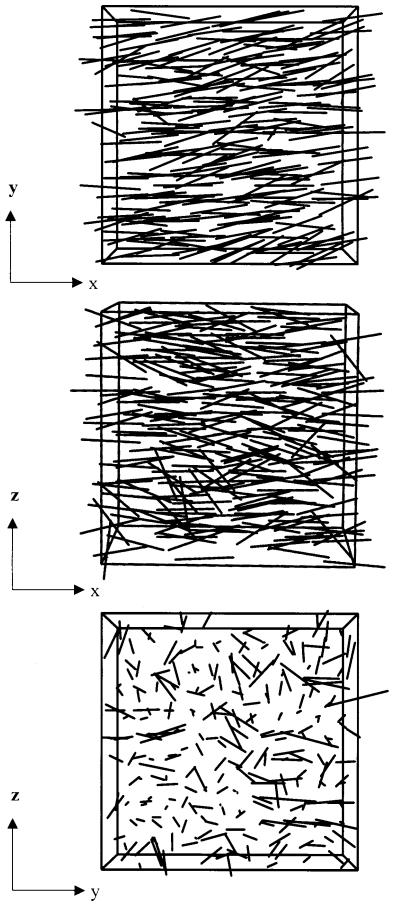

Figure 5. The steady-state snapshot projected to *xy*-, *xz*-, and *yz*-plane at 300 K, 1.386 g/cm^3, and γ= 8.0 ps^{-1}.

Table 3. The effect of density on the shear rate dependence of LJ-energy and order parameters at 300 K for N = 96 system. The Figures in parentheses are estimated (one standard deviation) errors in the quoted digits

ρ (g/cm^3)	γ (ps^{-1})	$\langle \mathbf{E}^{LJ}/N \rangle$ (kJ/mol)	$\langle S_2 \rangle$	$\langle S_4 \rangle$	$\langle S_6 \rangle$
1.243	2.000	-20.192(0.404)	0.735(0.042)	0.443(0.056)	0.230(0.054)
	1.000	-20.350(0.354)	0.608(0.047)	0.289(0.055)	0.112(0.049)
	0.100	-19.936(0.257)	0.199(0.046)		
	0.010	-19.856(0.275)	0.101(0.036)		
	0.001	-19.892(0.273)	0.124(0.054)		
	0.000	-19.870(0.259)	0.109(0.040)		
1.098	2.000	-17.830(0.409)	0.644(0.047)	0.342(0.058)	0.161(0.054)
	1.000	-17.991(0.372)	0.504(0.055)	0.200(0.065)	0.059(0.054)
	0.100	-17.807(0.339)	0.192(0.056)		
	0.010	-17.605(0.338)	0.125(0.041)		
	0.001	-17.823(0.310)	0.147(0.050)		
	0.000	-17.638(0.285)	0.101(0.033)		
1.056	2.000	-17.342(0.426)	0.651(0.040)	0.361(0.057)	0.168(0.058)
	1.000	-17.451(0.565)	0.494(0.057)	0.183(0.057)	0.054(0.049)
	0.100	-17.210(0.387)	0.177(0.058)		
	0.010	-17.077(0.361)	0.120(0.037)		
	0.001	-16.910(0.324)	0.119(0.046)		
	0.000	-17.338(0.449)	0.116(0.040)		
1.046	2.000	-17.135(0.386)	0.633(0.051)	0.320(0.057)	0.139(0.051)
	1.000	-17.160(0.407)	0.468(0.067)	0.193(0.061)	0.065(0.050)
	0.100	-16.938(0.317)	0.143(0.051)		
	0.010	-16.992(0.379)	0.116(0.032)		
	0.001	-16.928(0.417)	0.116(0.042)		
	0.000	-17.015(0.443)	0.097(0.035)		

Table 3. Continued

ρ (g/cm^3)	γ (ps^{-1})	$\langle \mathbf{E}^{LJ}/N \rangle$ (kJ/mol)	$\langle S_2 \rangle$	$\langle S_4 \rangle$	$\langle S_6 \rangle$
0.994	2.000	-16.248(0.463)	0.615(0.048)	0.311(0.061)	0.135(0.058)
	1.000	-16.754(0.456)	0.481(0.055)	0.191(0.058)	0.067(0.051)
	0.100	-16.374(0.459)	0.136(0.043)		
	0.010	-16.439(0.385)	0.107(0.038)		
	0.001	-16.229(0.405)	0.109(0.038)		
	0.000	-16.349(0.455)	0.119(0.042)		
0.747	2.000	-12.765(0.526)	0.487(0.051)	0.193(0.057)	0.075(0.049)
	1.000	-15.915(0.579)	0.437(0.057)	0.156(0.071)	0.050(0.053)
	0.100	-14.245(0.475)	0.125(0.046)		
	0.010	-14.316(0.488)	0.128(0.042)		
	0.001	-14.584(0.615)	0.112(0.048)		
	0.000	-14.505(0.450)	0.103(0.041)		

Table 4. The effect of temperature on the shear rate dependence of LJ-energy and order parameters at 0.994 g/cm^3 for N = 96 system. The Figures in parentheses are estimated (one standard deviation) errors in the quoted digits

T (K)	γ(ps^{-1})	$\langle \mathbf{E}^{LJ}/N \rangle$ (kJ/mol)	$\langle S_2 \rangle$	$\langle S_4 \rangle$	$\langle S_6 \rangle$
300.0	2.000	-16.248(0.463)	0.615(0.048)	0.311(0.061)	0.135(0.058)
	1.000	-16.754(0.456)	0.481(0.055)	0.191(0.058)	0.067(0.051)
	0.100	-16.374(0.459)	0.136(0.043)		
	0.010	-16.439(0.385)	0.107(0.038)		
	0.001	-16.229(0.405)	0.109(0.038)		
	0.000	-16.349(0.455)	0.119(0.042)		
290.0	2.000	-16.412(0.377)	0.610(0.048)	0.296(0.065)	0.125(0.062)
	1.000	-16.726(0.420)	0.475(0.092)	0.193(0.083)	0.075(0.056)
	0.100	-16.854(0.474)	0.117(0.037)		
	0.010	-16.862(0.504)	0.135(0.051)		
	0.001	-16.441(0.429)	0.132(0.038)		
	0.000	-16.749(0.511)	0.126(0.046)		
275.0	2.000	-16.609(0.521)	0.647(0.042)	0.337(0.055)	0.153(0.049)
	1.000	-17.189(0.512)	0.484(0.049)	0.183(0.045)	0.053(0.039)
	0.100	-17.181(0.489)	0.151(0.040)		
	0.010	-17.446(0.516)	0.111(0.037)		
	0.001	-17.468(0.511)	0.111(0.042)		
	0.000	-17.246(0.426)	0.132(0.035)		
250.0	2.000	-16.905(0.381)	0.652(0.041)	0.358(0.051)	0.168(0.056)
	1.000	-17.562(0.496)	0.509(0.050)	0.212(0.051)	0.076(0.050)
	0.100	-18.450(0.614)	0.157(0.064)		
	0.010	-18.706(0.631)	0.130(0.037)		
	0.001	-18.536(0.553)	0.131(0.036)		
	0.000	-18.514(0.554)	0.117(0.043)		
240.0	2.000	-17.225(0.506)	0.662(0.053)	0.376(0.060)	0.194(0.048)
	1.000	-18.867(0.528)	0.550(0.083)	0.269(0.075)	0.115(0.056)
	0.100	-19.502(0.610)	0.304(0.090)		
	0.010	-20.254(0.560)	0.282(0.067)		
	0.001	-19.646(0.474)	0.232(0.056)		
	0.000	-19.044(0.453)	0.128(0.046)		

dence of order parameter. Now we present the results of our simulation for the effects of density and temperature on the shear rate dependence of orientational order. For extensive calculations, the system size was reduced to N = 96. Table 3 shows the results of the shear rate dependence of orientational order for each density at 300 K. The simulation results for Lennard-Jones energy per particle and orientational order parameters of N = 96 is comparable to those of N = 256 at the same density. Within the statistical error limit, the order parameter for each density exhibits similar value at isotropic states which correspond to γ= 0. Table 3 indicates that highly ordered phases are easily induced by shear for the system of high density due to strong *inter*-molecular interactions. The order parameter S_2 increases with an increase of shear rate and jumps at a critical shear rate γ= 1.0 ps^{-1} like an isotropic-nematic phase transition. This apparent nature does not imply that the behavior of the system under shear control may be similar to the response of lyotropic liquid crystalline

system to the variation of concentration. Table 4 shows the shear rate dependence of orientational order for various temperatures at the same density of 0.994 g/cm^3. As temperature decreases, the system exhibits more ordered structure at high shear rates because of the reduced reorientational motion.

Conclusion

The main goal of this paper is to investigate the change of orientational structure of the system consisted of anisotropic particles under an external field. We used the simple shear flow as an example of external field and employed a rodlike molecule as a representative of the anisotropic particle. The rodlike molecule is composed of linearly connected 6-sites interacting via Lennard-Jones potential. For the study of shear-induced structure change, we carried out nonequilibrium molecular dynamics (NEMD) simulation for the Couette flows of rodlike molecules. The SLLOD algorithm with Lees-Edwards sliding brick boundary condition was implemented for the evolution of the system under the steady shear.

The system composed of the rodlike molecules exhibits the change of orientational structure, that is, isotropic-nematic transition at high shear rate. The nature of the ordered system developed from the isotropic phase by steady shear was elucidated via an analysis of order parameters, OPCFs, ODF, and snapshots of configurations. The orientational order of the system develops gradually with an increase of shear rate. We have also presented our simulation results for the effect of density and temperature on the shear rate dependence of orientational order. Highly ordered phase is easily induced by shear for the system with high density and low temperature.

References

1. Emsley, J. W.; Long, J. E.; Luckhurst, G. R.; Pedrielli, P. *Phys. Rev. E* **1999**, *60*, 1831.
2. Chandrasekhar, S. *Liquid Crystals*; Cambridge University Press: Cambridge, U. K., 1977.
3. de Gennes, P. G.; Prost, J. *The Physics of Liquid Crystals*, 2nd ed.; Clarendon Press: Oxford, U. K., 1994.
4. Vertogen, G.; de Jeu, W. H. *Thermotropic Liquid Crystals, fundamentals*; Springer-Verlag: Heidelberg, Germany, 1988.
5. For the electric field effects in liquid crystals see Blinov, L. M. In *Handbook of Liquid Crystal Research*; Collings, P. J., Patel, J. S., Eds.; Oxford University Press: New York, U. S. A., 1997; p 125. For the magnetic field effects in liquid crystals see chap. 3 of ref. 2.
6. (a) Evans, D. J.; Morris, G. P. *Statistical Mechanics of Non-equilibrium Liquids*; Academic Press: New York, U. S. A., 1990. (b) Evans, D. J.; Morris, G. P. *Comput. Phys. Rep*. **1984**, *1*, 297. (c) Sarman, S. S.; Evans, D. J.; Cummings, P. T. *Phys. Rep*. **1998**, *305*, 1. (d) For example, Khare, R.; de Pablo, J.; Yethiraj, A. *J. Chem. Phys*. **1997**, *107*, 6956.
7. Bennett, L.; Hess, S.; Borgmeyer, C. P.; Weider, T. *Int. J. Thermophys.* **1998**, *19*, 1143.
8. (a) Evans, D. J. *Mol. Phys.* **1977**, *34*, 317. (b) Evans, D. J.; Murad, S. *Mol. Phys.* **1977**, *34*, 327.
9. Allen, M. P.; Tildesley, D. J. *Computer Simulation of Liquids*; Clarendon Press: New York, U. S. A., 1987; Chap. 3.
10. Lees, A. W.; Edwards, S. F. *J. Phys. C*: *Solid State Phys*. **1972**, *5*, 1921.
11. Gear, C. W. *Numerical Initial Value Problems in Ordinary Differential Equations*; Prentice-Hall: New Jersey, U. S. A., 1971.
12. Zannoni, C. In *The Molecular Physics of Liquid Crystals*; Luckhurst, G. R., Gray, G. W., Eds.; Academic Press: New York, U. S. A., 1979; chap. 3 and chap. 9.